Analysis of Guided Modes in Multilayer/Multiconductor Structures by the "Boundary Integral—Resonant Mode Expansion Method"

Marco Bressan, *Member, IEEE*, Giuseppe Conciauro, *Member, IEEE*, and Paolo Gamba, *Member, IEEE*

Abstract—**This paper describes a new method for the analysis of modes propagating in shielded waveguides consisting of many dielectric and perfectly conducting layers of different widths. The eigenvalue problem inherent to the mode determination is formulated subdividing the structure into layered elementary wave-guides (EWG's) and matching the fields generated in adjacent EWG's by unknown equivalent sources placed at the interfaces. The special representation of the EWG field, consisting of boundary integrals and mode expansions, leads to a linear matrix eigenvalue problem involving a limited number of variables. Thanks to this peculiarity the method permits to determine many modes in short computing times. The method was implemented in a flexible and fully automatic computer code, whose reliability and efficiency has been confirmed by many tests.**

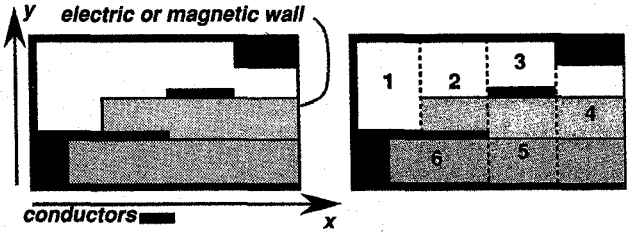

(a) (b)

Fig. 1. (a) Cross section of a multilayer/multiconductor waveguide. (b) Subdivision of the cross section into rectangular regions containing an x-invariant medium.

I. Introduction

With the development of integrated circuits operating at microwave, millimeter-wave, and optical frequencies, a great effort has been devoted to invent more and more efficient algorithms for the full-wave analysis of multilayered waveguides of ever-increasing complexity. A number of waveguides of practical interest consist of many dielectric and conducting layers of different widths enclosed in a rectangular shield [Fig. 1(a)]. Therefore, a general computer code for the modal analysis of this class of structures can be very useful. Reliability and efficiency in multimode analysis are required, since many modes often propagate in the operating band of complex waveguides.

Recently many two-dimensional (2-D) time-domain algorithms have been developed for the dispersion analysis of complex waveguides [1]–[7]. These algorithms loose their efficiency in multimode analysis, due to the necessity of considering a very large number of time steps to resolve, in the frequency domain, modes propagating at close frequencies with the same phase constant.

Other algorithms, based on the mode-matching, the transverse resonance or the boundary integral method have been used extensively for studying particular structures belonging to the considered class and, recently, for implementing some general purpose codes [8]–[11]. In these methods the dispersion analysis requires to recalculate many and many times the system matrix in order to locate the zeros of its determinant in the ω-β plane. In multimode analysis this makes these methods time-consuming and unsuitable for automatization, since some human control is necessary to be sure not to miss some modes.

In two recent conference papers [12], [13] we gave a rough description of a novel method that leads to the mode determination by the solution of a *linear* matrix eigenvalue problem involving a reasonably small number of variables. This permits a dramatic saving in computing time and removes the risk of missing modes. The present paper is intended to describe the method in the necessary detail, including some improvements which avoid the spurious solutions that, in the early version, were found at (nominally) zero frequency [12]. Here the method is named "boundary integral-resonant mode expansion (BI-RME) method," due to the particular form of the field representation.

In Section II, we describe the theory and report the formulas that are strictly necessary for a clear understanding of the method; in Section III we give some informations on the numerical implementation and report some result; in Section IV we discuss the advantages of the method.

II. Theory

We consider lossless isotropic waveguides [Fig. 1(a)] bounded by electric walls and, possibly, by one magnetic wall on one side (considering the magnetic wall is useful for studying symmetric structures). We restrict our analysis

Manuscript received December 22, 1994; revised January 17, 1996. This work was supported by MURST and by CNR (ST93.04769.74).

The authors are with the Department of Electronics of the University of Pavia, Pavia, Italy.

Publisher Item Identifier S 0018-9480(96)03022-0.

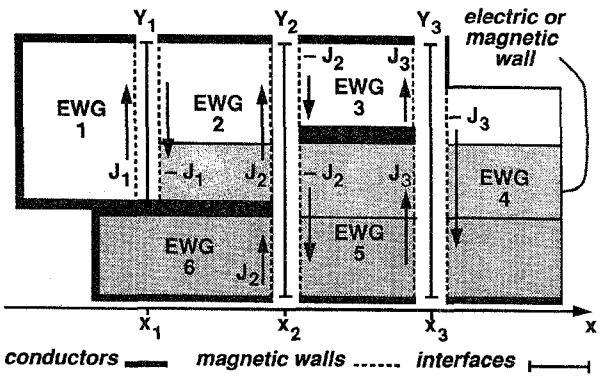

Fig. 2. Subdivision of the structure into EWG's excited by the equivalent current sheets defined over the interfaces.

to propagating (noncomplex) modes, i.e., to fields depending on the factor $\exp j(\omega t - \beta z)$, with $\beta > 0$. As usual in modal analysis this factor is understood and the field is studied in two dimensions. For any given value of β we determine the frequencies and the fields for all modes propagating below some frequency $\omega_{\max}$. Then, in the eigenvalue problem inherent to the mode determination, the frequency ω plays the role of the eigenvalue and the modes are determined as 2-D resonant modes depending on the parameter β.

As shown in Fig. 1(b), the cross section consists of a number of interconnected rectangular regions, each containing a x-invariant dielectric and bounded by electric walls on the top, on the bottom and, possibly, on one side. As shown in Fig. 2 we isolate these regions introducing a set of fictitious magnetic walls, thus subdividing the waveguide into elementary waveguides (EWG's), numbered from one to M. Furthermore, according to the equivalence theorem, we introduce on the fictitious magnetic walls some traveling-wave current sheets propagating in the z-direction with the phase constant β, in such a way as to generate, in all the EWG's, fields propagating with the same phase constant as the modes we want to determine. As shown in the figure, the currents densities on adjacent magnetic walls are opposite, in order to assure the continuity of the tangential component of the magnetic field in adjacent EWG's.

The union of all the fictitious magnetic walls consists of N separate segments $Y_1, Y_2, \cdots, Y_N$ (see Fig. 2). These segments, named "interfaces," consist of points placed on magnetic walls of adjacent EWG's and, possibly, on lateral boundaries of conductors. The current on the left and the right of the interface Y_n are denoted by $\vec{J}_n$ and $-\vec{J}_n$ respectively (note that only $\vec{J}_n$ or $-\vec{J}_n$ is present where the interface touches a conductor). In any case, one function $\vec{J}_n = \vec{J}_n(y)$, defined over Y_n, is sufficient to describe all the equivalent currents on the left and/or on the right of the interface, so that the set of functions $\vec{J}_1, \vec{J}_2, \cdots, \vec{J}_N$, completely describes all the equivalent currents in the EWG's.

The EWG's are bounded at the top and the bottom by electric walls and, laterally, by a pair of magnetic walls or by an electric and a magnetic wall. They all include a dielectric medium layered in the y-direction only. Then, the EWG's are simple enough for representing analytically the field generated by the equivalent currents. The form of the eigenvalue problem, that is formulated by enforcing the continuity of tangential electric field at the interfaces, depends on the way we represent the EWG field. The boundary integral-resonant mode expansion (BI-RME) representation discussed below leads to a linear eigenvalue problem.

A. BI-RME Representation of the EWG Field

Let us consider the mth EWG and assume that it is included within two interfaces—say Y_n on the left and $Y_{n'}$ on the right—placed at the abscissas x_n and $x_{n'}$ [Fig. 3(a)]. Let us denote by ϵ^m and μ^m the electric and magnetic permittivities of the medium, that are piecewise-constant function of y, defined in the interval Y^m spanned by the EWG. Finally, let us introduce the surface charge densities ρ_n and $\rho_{n'}$ associated to J_n and $J_{n'}$. These densities are given by

$$\rho_n = -\frac{\nabla_{yz} \cdot \vec{J}_n}{j\omega} \qquad (\nabla_{yz} \stackrel{\text{def}}{=} \vec{u}_y \partial_y - j\beta \vec{u}_z). \tag{1}$$

The field in the EWG can be represented as follows [12]:

$$\vec{E}^m = -\nabla V^m - j\omega \vec{A}^m + \omega^2 \sum_{p,q} \left(\frac{a'^m_{pq} \vec{e}'^m_{pq}}{\omega'^{m2}_{pq}} + \frac{a''^m_{pq} \vec{e}''^m_{pq}}{\omega''^{m2}_{pq}} \right) \tag{2}$$

$$\vec{H}^m = \frac{\nabla \times \vec{A}^m}{\mu^m} + \frac{j\omega}{\mu^m} \sum_{p,q} \left(\frac{a'^m_{pq} \nabla \times \vec{e}'^m_{pq}}{\omega'^{m2}_{pq}} + \frac{a''^m_{pq} \nabla \times \vec{e}''^m_{pq}}{\omega''^{m2}_{pq}} \right) \tag{3}$$

where $\nabla = \vec{u}_x \partial_x + \vec{u}_y \partial_y - j\beta \vec{u}_z$; V^m and $\vec{A}^m$ are the quasi-static scalar and vector potentials; ω'^m_{pq}, $\vec{e}'^m_{pq}$ and ω''^m_{pq}, $\vec{e}''^m_{pq}$ are the frequencies and the electric fields for the LSM_{pq} and LSE_{pq} modes of the EWG, propagating with the phase constant β; a'^m_{pq} and a''^m_{pq} are the mode amplitudes. Assuming the normalization $\int\int \epsilon \vec{e} \cdot \vec{e}^*\, dx\, dy = 1$, the amplitudes of both types of modes satisfy the equation

$$a^m_{pq} = \frac{-j\omega}{\omega^{m2}_{pq} - \omega^2} \left(\int_{Y^m} \vec{e}^{m*}_{pq}(x_{n'}, y) \cdot \vec{J}_{n'}(y)\, dy - \int_{Y^m} \vec{e}^{m*}_{pq}(x_n, y) \cdot \vec{J}_n(y)\, dy \right). \tag{4}$$

The potentials are represented by the boundary integrals

$$V^m(x,y) = \int_{Y^m} g^m(x, y, x_{n'}, y') \rho_{n'}(y')\, dy' - \int_{Y^m} g^m(x, y, x_n, y') \rho_n(y')\, dy' \tag{5}$$

$$\vec{A}^m(x,y) = \int_{Y^m} \overleftrightarrow{G}^m(x, y, x_{n'}, y') \cdot \vec{J}_{n'}(y')\, dy' - \int_{Y^m} \overleftrightarrow{G}^m(x, y, x_n, y') \cdot \vec{J}_n(y')\, dy' \tag{6}$$

where g^m and $\overleftrightarrow{G}^m$ are the Green's functions for the quasi-static scalar and vector potentials in the EWG. Equations (2) and (3) hold true also when the EWG borders on one interface

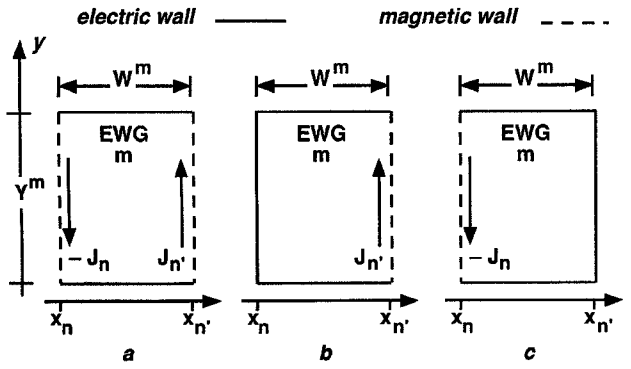

Fig. 3. Possible EWG lateral boundaries. (a) Magnetic-magnetic walls. (b) and (c) Magnetic-electric wall.

only [Fig. 3(b) and (c)] but, in this case, one of the integrals in (4)–(6) is missing.

The series in (2) and (3) involve the modes of the EWG considered with the same phase constant, at different propagating frequencies. In other words, these modes are considered as transversely resonant modes, their propagating frequencies having the meaning of resonant frequencies. In this sense these series represent "resonant mode expansions." We see that (2) and (3) constitute a hybrid representation consisting of boundary integrals (BI) and of resonant mode expansions (RME). The quasi-static boundary integrals permit an accurate representation of the field near the interfaces, where the field varies rapidly due to the discontinuity of the medium and to the presence of metallic and/or dielectric edges [14]; in fact the discontinuities and the singularities of the field obey the same laws in the quasi-static and in the high-frequency case, so that the rapid variations of the field can be accurately reproduced provided the currents on the interface are allowed to vary rapidly. The resonant mode expansions represent a much smoother field, because the contributions of the highest order modes become rapidly unimportant (asymptotically, they depend on the factor $(\omega_{pq}^m)^{-4}$). Then, the RME can be truncated, retaining a limited number of the lowest order modes, say those satisfying

$$\omega_{pq}^{\prime m}, \omega_{pq}^{\prime\prime m} < \zeta \omega_{\max} \tag{7}$$

with ζ not much larger than one (in Section III we shall see that considering $\zeta > 2.5$ is sufficient). Note that the number of retained modes is small if the dimensions of the EWG are not much larger than the wavelength at the frequency $\zeta\omega_{\max}$.

The modal electric fields and the Green's functions have the form

$$\vec{e}_{pq}^{\prime m} = \frac{\mathcal{M}_p^m \Psi_{pq}^m}{\epsilon^m \omega_{pq}^{\prime m} \beta_p^m} \qquad \vec{e}_{pq}^{\prime\prime m} = \frac{\mathcal{N}_p^m \Phi_{pq}^m}{\beta_p^m} \tag{8}$$

$$g^m = \sum_{p=0}^{\infty} \xi_p^m(x) \xi_p^m(x') F_p^m(y, y') \tag{9}$$

$$\overleftrightarrow{G}^m = \sum_{p=0}^{\infty} \left(\frac{\mathcal{M}_p^m \mathcal{M}_p^{m\prime *} S_p^m(y, y')}{\beta_p^{m2} \epsilon^m(y) \epsilon^m(y')} + \frac{\mathcal{N}_p^m \mathcal{N}_p^{m\prime *} R_p^m(y, y')}{\beta_p^{m2}} \right) \tag{10}$$

TABLE I
EXPRESSIONS OF $\nu_p^m, \beta_p^m, \xi_p^m(x), \chi_p^m(x)$
($X^m = x - x_n; p = 0, 1, \cdots; \delta_{0p}$ = KRONECKER INDEX)

	EWG type		
	Fig. 3a	Fig. 3b	Fig. 3c
ν_p^m	$p\pi/W^m$	$(p+1/2)\pi/W^m$	
ξ_p^m	$\sqrt{\frac{2-\delta_{0p}}{W^m}} \cos(\nu_p^m X^m)$	$\sqrt{\frac{2}{W^m}} \sin(\nu_p^m X^m)$	$\sqrt{\frac{2}{W^m}} \cos(\nu_p^m X^m)$
χ_p^m	$-\sqrt{\frac{2}{W^m}} \sin(\nu_p^m X^m)$	$\sqrt{\frac{2}{W^m}} \cos(\nu_p^m X^m)$	$-\sqrt{\frac{2}{W^m}} \sin(\nu_p^m X^m)$
β_p^m	$\sqrt{\nu_p^{m2} + \beta^2}$		

where

$$\mathcal{M}_p^m = \vec{u}_x \nu_p^m \chi_p^m(x) \partial_y + \xi_p^m(x)(\vec{u}_y \beta_p^{m2} - j\vec{u}_z \beta \partial_y)$$
$$\mathcal{N}_p^m = \vec{u}_x \beta \chi_p^m(x) + j\vec{u}_z \nu_p^m \xi_p^m(x). \tag{11}$$

The symbols $\nu_p^m, \beta_p^m, \xi_p^m(x), \chi_p^m(x)$ are defined in Table I; $\mathcal{M}_p^{m\prime *}$ and $\mathcal{N}_p^{m\prime *}$ represent the conjugate of $\mathcal{M}_p^m$ and $\mathcal{N}_p^m$ with x, y replaced by x', y'. The other functions in (8)–(10) result from the solution of the following equations:

$$\partial_y(1/\epsilon^m)\partial_y \Psi_{pq}^m - (\beta_p^{m2}/\epsilon^m - \mu^m \omega_{pq}^{\prime m2})\Psi_{pq}^m = 0 \tag{12}$$
$$\partial_y(1/\mu^m)\partial_y \Phi_{pq}^m - (\beta_p^{m2}/\mu^m - \epsilon^m \omega_{pq}^{\prime\prime m2})\Phi_{pq}^m = 0 \tag{13}$$

$$\partial_y \epsilon^m \partial_y F_p^m - \beta_p^{m2} \epsilon^m F_p^m = -\delta(y - y') \tag{14}$$
$$\partial_y(1/\mu^m)\partial_y R_p^m - (\beta_p^{m2}/\mu^m) R_p^m = -\delta(y - y') \tag{15}$$
$$\partial_y(1/\epsilon^m)\partial_y S_p^m - (\beta_p^{m2}/\epsilon^m) S_p^m = -\mu^m T_p^m \tag{16}$$
$$\partial_y(1/\epsilon^m)\partial_y T_p^m - (\beta_p^{m2}/\epsilon^m) T_p^m = -\delta(y - y') \tag{17}$$

$$\left.\begin{array}{lll} \Phi_{pq}^m = 0 & F_p^m = 0 & R_p^m = 0 \\ \partial_y \Psi_{pq}^m = 0 & \partial_y S_p^m = 0 & \partial_y T_p^m = 0 \end{array}\right\} \text{ at the extremes of } Y^m$$

$$\int_{Y^m} \mu^m \Psi_{pq}^{m\,2}\, dy = 1 \qquad \int_{Y^m} \epsilon^m \Phi_{pq}^{m\,2}\, dy = 1. \tag{18}$$

The equations (12) and (13), where $\omega_{pq}^{\prime m}$ and $\omega_{pq}^{\prime\prime m}$ play the role of eigenvalues, result from the study of the LSM and LSE modes by the method of variable separation. For any value of p, the index q labels the eigensolutions in the nondecreasing order of the eigenvalues. Equation (14) derives from the solution of $\nabla \cdot \epsilon \nabla g = -\delta(x - x')\delta(y - y')$ with the Dirichelet and Neumann boundary conditions on the electric and the magnetic walls, respectively. The origin of (10), (15), (16), and (17) is discussed in Appendix A.

Note that the Green's functions F_p^m, R_p^m, T_p^m, and S_p^m can be determined in closed form; therefore, for any EWG, g^m and $\overleftrightarrow{G}^m$ are available in the form of one-index series. The general expressions of the Green's functions are reported in Table II (the superscript m is omitted). The coefficients $a_{ij}, b_{ij}, \cdots$ in the table depend on the layers i and j where the observation and the source points are placed. They are determined enforcing the boundary conditions and the continuity of $F_p, \epsilon\partial_y F_p, R_p, \mu^{-1}\partial_y R_p, S_p, \epsilon^{-1}\partial_y S_p$ at the interfaces between the layers. The table also includes the general expression of the eigenfunctions. The coefficients A_i' B_i' A_i'' B_i'', that

TABLE II

GENERAL FORMS OF THE GREEN'S FUNCTIONS AND THE EIGENFUNCTIONS THE LAYERS OF THE EWG ARE NUMBERED IN THE INCREASING ORDER FROM THE BOTTOM; THE iTH LAYER HAS THE PERMITTIVITIES ϵ_i, μ_i AND IT SPANS THE INTERVAL $[y_{i-1}, y_i]$; THE OBSERVATION AND THE SOURCE POINTS, y AND y' ARE PLACED IN THE i-TH AND IN THE jTH LAYER, RESPECTIVELY SYMBOLS. $\underline{y} = y - y_{i-1}, \overline{y} = y_i - y, \underline{y}' = y' - y_{j-1}, \overline{y}' = y_j - y'; \delta_{ij} =$ KRONECKER INDEX, $a_{ij}, b_{ij}, c_{ij}, d_{ij}, f_{ij}, g_{ij}, r_{ij}, s_{ij}, t_{ij}, A'_i, B'_i, A''_i, B''_i =$ COEFFICIENTS TO BE DETERMINED

$$F_p = \delta_{ij}\frac{e^{-\beta_p|y-y'|}}{2\beta_p\epsilon_j} + a_{ij}e^{-\beta_p(\underline{y}+\underline{y}')} + b_{ij}e^{-\beta_p(\underline{y}+\overline{y}')} + b_{ji}e^{-\beta_p(\overline{y}+\underline{y}')} + c_{ij}e^{-\beta_p(\overline{y}+\overline{y}')}$$

$$R_p = \delta_{ij}\frac{\mu_j e^{-\beta_p|y-y'|}}{2\beta_p} + d_{ij}e^{-\beta_p(\underline{y}+\underline{y}')} + f_{ij}e^{-\beta_p(\underline{y}+\overline{y}')} + f_{ji}e^{-\beta_p(\overline{y}+\underline{y}')} + g_{ij}e^{-\beta_p(\overline{y}+\overline{y}')}$$

$$T_p = \delta_{ij}\frac{\epsilon_j e^{-\beta_p|y-y'|}}{2\beta_p} - \epsilon_i\epsilon_j\left(a_{ij}e^{-\beta_p(\underline{y}+\underline{y}')} - b_{ij}e^{-\beta_p(\underline{y}+\overline{y}')} - b_{ji}e^{-\beta_p(\overline{y}+\underline{y}')} + c_{ij}e^{-\beta_p(\overline{y}+\overline{y}')}\right)$$

$$S_p = \delta_{ij}\epsilon_i^2\mu_i\frac{2(1+\beta_p|y-y'|)e^{-\beta_p|y-y'|} - e^{-\beta_p(\underline{y}+\underline{y}')} - e^{-\beta_p(\overline{y}+\overline{y}')}}{8\beta_p^3} + \frac{\epsilon_i\epsilon_j}{2\beta_p^2}\Big[\left(r_{ij} - a_{ij}\beta_p(\epsilon_i\mu_i\underline{y} + \epsilon_j\mu_j\underline{y}')\right)e^{-\beta_p(\underline{y}+\underline{y}')} +$$
$$\left(s_{ij} + b_{ij}\beta_p(\epsilon_i\mu_i\underline{y} + \epsilon_j\mu_j\overline{y}')\right)e^{-\beta_p(\underline{y}+\overline{y}')} + \left(s_{ji} + b_{ji}\beta_p(\epsilon_i\mu_i\overline{y} + \epsilon_j\mu_j\underline{y}')\right)e^{-\beta_p(\overline{y}+\underline{y}')} + \left(t_{ij} - c_{ij}\beta_p(\epsilon_i\mu_i\overline{y} + \epsilon_j\mu_j\overline{y}')\right)e^{-\beta_p(\overline{y}+\overline{y}')}\Big]$$

$$\Psi_{pq} = \left(A'_i\cos\kappa_i\underline{y} + B'_i\cos\kappa_i\overline{y}\right)_{\omega=\omega'_{pq}} \qquad \Phi_{pq} = \left(A''_i\sin\kappa_i\underline{y} + B''_i\sin\kappa_i\overline{y}\right)_{\omega=\omega''_{pq}} \qquad \left(\kappa_i = \sqrt{\omega^2\epsilon_i\mu_i - \beta_p^2}\right)$$

depend on the layer, are determined enforcing the continuity of $\Psi_{pq}, \epsilon^{-1}\partial_y\Psi_{pq}, \Phi_{pq}, \mu^{-1}\partial_y\Phi_{pq}$ between the layers, the boundary conditions and the normalization (18). The resulting equations also play the role of characteristic equations for the determination of the resonant frequencies of the LSM and LSE modes. With no more than three layers it is sufficiently easy to find the analytical expressions of the characteristic equations and of the coefficients involved in the Green's functions and in the eigenfunctions. These expressions are not reported for brevity.

B. Representation of the Charge and Current Densities

The current density at each interface shall be approximated using a finite set of basis functions. The choice of this set is crucial to avoid spurious solutions.

We note that solenoidal currents ($\nabla_{yz}\cdot\vec{J}_n = 0$) would generate in the EWG's electric fields where the term ∇V is missing (because $\rho_n = 0$ and $V = 0$). Then, looking at (2), we realize at glance that such currents would generate in the EWG's an electric field going to zero for $\omega \to 0$. This implies that matching the electric field at the interfaces we obtain a set of equations that, for $\omega = 0$, is satisfied identically by any set of solenoidal currents. Evidently these solutions are meaningless.

If the span of the chosen basis includes solenoidal currents, we shall find as many meaningless solutions as the number of independent solenoidal currents that our basis permits to represent; these solutions, indeed, could be easily detected and disregarded, they being marked by the zero eigenvalue. On the other hand, if solenoidal currents are outside the span of the basis, the said solutions would be found only approximately, so that they will appear with nonzero eigenvalues, making their detection difficult or impossible. Then, for avoiding spurious solutions it is necessary to choose a basis whose span includes solenoidal functions. Furthermore, as shown below, this choice permits to formulate the final eigenvalue problem in such a way as not to meet the zero eigenvalue at all.

In order to permit the representation of solenoidal currents the functions $\partial_y(\vec{J}_n)_y$ and $-j\beta(\vec{J}_n)_z$ are approximated in the same basis. Thus, considering K_n functions $b_{n1}, b_{n2}, \cdots, b_{nK_n}$ defined on the interface Y_n and such that their derivatives constitute a suitable basis for $\partial_y(\vec{J}_n)_y$ and $(\vec{J}_n)_z$, we introduce the approximations

$$(\vec{J}_n)_y = \int \partial_y(\vec{J}_n)_y\, dy = \kappa_n i_{n0} + \sum_{k=1}^{K_n}(\beta i_{nk} - j\omega q_{nk})b_{nk} \tag{19}$$

$$(\vec{J}_n)_z = -j\sum_{k=1}^{K_n} i_{nk}\dot{b}_{nk} \tag{20}$$

where i_{nk} and q_{nk} are unknown coefficients, κ_n is some constant having the same dimensions of β and $\dot{b}_{nk} = \partial_y b_{nk}$. It is noted that, according to (1), we have

$$\rho_n = \sum_{k=1}^{K_n} q_{nk}\dot{b}_{nk} \tag{21}$$

so that $\vec{J}_n$ is solenoidal when the q-coefficients are zero. Equations (19) and (20) can be rewritten as

$$\vec{J}_n = -j\omega\sum_{k=1}^{K_n}\vec{v}_{nk}q_{nk} + \sum_{h=O}^{K_n}\vec{w}_{nh}i_{nh} \tag{22}$$

where we introduced the vector base functions

$$\vec{v}_{nk} = b_{nk}\vec{u}_y$$
$$\vec{w}_{nh} = \beta b_{nh}\vec{u}_y - j\dot{b}_{nh}\vec{u}_z \qquad (h \neq 0)$$
$$\vec{w}_{n0} = \kappa_n\vec{u}_y.$$

Note that the w-functions are solenoidal.

C. The Eigenvalue Problem

Let $\vec{E}_n^-$ and $\vec{E}_n^+$ be the electric fields on the left and the right of the interface Y_n. Using the Galerkin method we match their tangential components enforcing the conditions

$$\int_{Y_n} \vec{v}_{nk}^* \cdot (\vec{E}_n^+ - \vec{E}_n^-)\, dy = 0$$
$$\int_{Y_n} \vec{w}_{nh}^* \cdot (\vec{E}_n^+ - \vec{E}_n^-)\, dy = 0$$
$$k = 1, 2, \cdots, K_n \quad h = 0, 1, \cdots, K_n.$$

Over the parts of the interface bordering on the left (right) with EWG's the field $\vec{E}_n^-$ ($\vec{E}_n^+$) correspond to the field in these EWGs; in the remaining parts (if any) the tangential components of $\vec{E}_n^-$ or $\vec{E}_n^+$ are zero, these parts bordering on the lateral boundaries of conductors. Therefore the preceding equations may be put into the form

$$\sum_{m=1}^{M} \delta_n^m \int_{Y^m} \vec{v}_{nk}^*(y) \cdot \vec{E}^m(x_n, y)\, dy = 0 \tag{23}$$

$$\sum_{m=1}^{M} \delta_n^m \int_{Y^m} \vec{w}_{nh}^*(y) \cdot \vec{E}^m(x_n, y)\, dy = 0 \tag{24}$$

where $\delta_n^m \neq 0$ only when the mth EWG borders on Y_n; more specifically, $\delta_n^m = -1$ or $\delta_n^m = 1$ when the EWG is placed on the left or on the right of Y_n, respectively. We have as many equations of the type (23) as many functions $\vec{v}$ we have defined in all interfaces, i.e., $K = \Sigma\, K_n$. The number of the equations of the type (24) is $H = K + N$, since the number of w-functions on each interface exceed by one that of the v-functions.

Introducing (2) into (23) and (24) we obtain two systems of algebraic equations involving all the unknown coefficients q_{nk}, i_{nh} and all the mode amplitudes of the LSM and LSE modes retained in the BI-RME representations of the EWG fields. These systems, written in matrix form, are

$$\boldsymbol{F}\boldsymbol{q} - j\omega\boldsymbol{T}\boldsymbol{i} - \omega^2(\boldsymbol{S}\boldsymbol{q} - \boldsymbol{V}\boldsymbol{\Omega}^{-2}\boldsymbol{a}) = 0 \tag{25}$$

$$-j\omega[\boldsymbol{R}\boldsymbol{i} - j\omega(\tilde{\boldsymbol{T}}\boldsymbol{q} - \boldsymbol{W}\boldsymbol{\Omega}^{-2}\boldsymbol{a})] = 0 \tag{26}$$

where: the vectors $\boldsymbol{q}$ and $\boldsymbol{i}$ include in some order all the q- and i-coefficients pertaining to all interfaces; the vector $\boldsymbol{a}$ includes in some order the amplitudes of all the LSM and LSE modes retained in the BI-RME representation of the EWG fields; $\boldsymbol{\Omega}$ is the diagonal matrix including all the resonant frequencies, in the same order as the mode amplitudes in $\boldsymbol{a}$; the symbols $\boldsymbol{F}, \boldsymbol{R}, \boldsymbol{S}, \boldsymbol{T}, \boldsymbol{V}$, and $\boldsymbol{W}$ represent the matrices defined in Table III and the tilde denotes the transpose. In deriving (26) we used the identity

$$\int_{Y^m} \vec{w}_{nh'}^*(y) \cdot \nabla_{yz} V^m(x_n, y)\, dy = 0$$

that is valid because $\vec{w}$ is solenoidal and V is zero at the extremes of Y^m.

The matrix elements are reported in Table III, both in the form that results directly from (23) and (24) and in terms of the scalar basis functions. The second form—useful for calculations—is obtained integrating by parts, with some manipulations involving (12)–(17). It is stressed that all matrices are real and frequency independent and that $\boldsymbol{F}, \boldsymbol{R}$, and $\boldsymbol{S}$ are square, symmetric, and positive definite (see Appendix B).

Another system of equations derives from (4), after multiplication by $\omega_{pq}^{m2} - \omega^2$ and substitution of (22). In matrix form we have

$$\boldsymbol{\Omega}^2\boldsymbol{a} + j\omega\tilde{\boldsymbol{W}}\boldsymbol{i} + \omega^2(\tilde{\boldsymbol{V}}\boldsymbol{q} - \boldsymbol{a}) = 0. \tag{27}$$

Equations (25)–(27) are satisfied by any $\boldsymbol{i}$ if $\omega = 0, \boldsymbol{q} = 0, \boldsymbol{a} = 0$. This is the class of meaningless solutions we discussed in the previous subsection. The occurrence of these solutions depends on the existence of the factor $j\omega$ on the left-hand side of (26). Omitting this factor the spurious solutions are cut off, and the said equation permits to express the variable $\boldsymbol{i}$ as a function of the variables $\boldsymbol{q}$ and $\boldsymbol{a}$

$$\boldsymbol{i} = j\omega\boldsymbol{R}^{-1}(\tilde{\boldsymbol{T}}\boldsymbol{q} - \boldsymbol{W}\boldsymbol{\Omega}^{-2}\boldsymbol{a}). \tag{28}$$

Substituting into (25) and (27) we obtain the eigenvalue equation

$$\begin{pmatrix} \boldsymbol{A} & \boldsymbol{C} \\ \tilde{\boldsymbol{C}} & \boldsymbol{B} \end{pmatrix} \begin{pmatrix} \boldsymbol{q} \\ \boldsymbol{a} \end{pmatrix} = \omega^{-2} \begin{pmatrix} \boldsymbol{F} & 0 \\ 0 & 1 \end{pmatrix} \begin{pmatrix} \boldsymbol{q} \\ \boldsymbol{a} \end{pmatrix} \tag{29}$$

where

$$\boldsymbol{A} = \boldsymbol{S} - \boldsymbol{T}\boldsymbol{R}^{-1}\tilde{\boldsymbol{T}} \tag{30}$$

$$\boldsymbol{B} = \boldsymbol{\Omega}^{-2} - \boldsymbol{\Omega}^{-2}\tilde{\boldsymbol{W}}\boldsymbol{R}^{-1}\boldsymbol{W}\boldsymbol{\Omega}^{-2} \tag{31}$$

$$\boldsymbol{C} = (\boldsymbol{T}\boldsymbol{R}^{-1}\boldsymbol{W} - \boldsymbol{V})\boldsymbol{\Omega}^{-2}. \tag{32}$$

The eigenvalue equation is linear, because the matrices do not depend on ω. Note that this result has been obtained using as variables $\boldsymbol{q}$ and $\boldsymbol{a}$ (i.e., the charge densities at the interfaces and the modes of the EWG's). Of course, should we eliminate $\boldsymbol{q}$ or $\boldsymbol{a}$, the resulting eigenvalue problem would be nonlinear.

The matrices in (29) are real symmetric and the one on the right-hand side is evidently positive definite, due to the positive definiteness of $\boldsymbol{F}$. Also the matrix on the left-hand side is positive definite, since it can be shown that, for any set of equivalent sources (i.e., for any $(\boldsymbol{q}, \boldsymbol{a}) \neq 0$), we have

$$\omega^2(\tilde{\boldsymbol{q}} \quad \tilde{\boldsymbol{a}}) \begin{pmatrix} \boldsymbol{A} & \boldsymbol{C} \\ \tilde{\boldsymbol{C}} & \boldsymbol{B} \end{pmatrix} \begin{pmatrix} \boldsymbol{q} \\ \boldsymbol{a} \end{pmatrix} = \iint_{\substack{\text{cross} \\ \text{section}}} \mu\vec{H} \cdot \vec{H}^*\, dx\, dy > 0 \tag{33}$$

where $\vec{H}$ is given, for any EWG, by (3) (the demonstration is omitted for brevity). Due to the properties of the matrices, the eigenvalues are positive, so that the propagating frequencies of the modes are real, in spite of the approximation of the method.

We recall that the truncation of the RME in (2) and (3) is performed in such a way as to assure a good accuracy of the

TABLE III

MATRIX COEFFICIENTS THE INDEX $\imath$ DENOTES THE POSITION OF THE COEFFICIENT q_{lk} IN THE VECTOR $\boldsymbol{q}$; THE INDEX $\jmath$ DENOTES THE POSITION OF THE COEFFICIENT $\imath_{nh}$ IN THE VECTOR $\boldsymbol{i}$; THE INDEX r DENOTES THE POSITION OF THE AMPLITUDE a_{pq}^{lm} OR $a_{pq}^{l'm}$ IN THE VECTOR $\boldsymbol{a}$. THEN THE ORDERING OF THE VECTORS DEFINES THE FUNCTIONS. $l = l(\imath), k = k(\imath), n = n(\jmath), h = h(\jmath), m = m(\imath), p = p(r), q = q(r)$ THE PRIME IN THE INDICES DENOTES $l' = l(\imath'), k' = k(\imath')$ AND SO ON. THE PRIME IN THE FUNCTIONS DENOTES THE DEPENDENCE ON THE VARIABLE y'

$$\mathbf{F}_{\imath\imath'} = \sum_{m=1}^{M} \delta_l^m \delta_{l'}^m \iint_{Y^m} \nabla_{yz}^* \cdot \vec{v}_{lk}^* \, g^m(x_l, y, x_{l'}, y') \, \nabla_{y'z} \cdot \vec{v}'_{l'k'} \, dy dy' = \sum_{m=1}^{M} \sum_{p=0}^{\infty} (\delta_l^m \delta_{l'}^m)^{p+1} \sigma_p^m \iint_{Y^m} \dot{b}_{lk} \, F_p^m \, \dot{b}'_{l'k'} \, dy dy'$$

$$\mathbf{S}_{\imath\imath'} = \sum_{m=1}^{M} \delta_l^m \delta_{l'}^m \iint_{Y^m} \vec{v}_{lk}^* \cdot \vec{G}^m(x_l, y, x_{l'}, y') \cdot \vec{v}'_{l'k'} \, dy dy' = \sum_{m=1}^{M} \sum_{p=0}^{\infty} (\delta_l^m \delta_{l'}^m)^{p+1} \sigma_p^m \beta_p^{m2} \iint_{Y^m} \frac{b_{lk} S_p^m b'_{l'k'}}{\epsilon^m \epsilon'^m} \, dy dy'$$

$$\mathbf{T}_{\imath\jmath'} = \sum_{m=1}^{M} \delta_l^m \delta_{n'}^m \iint_{Y^m} \vec{v}_{lk}^* \cdot \vec{G}^m(x_l, y, x_{n'}, y') \cdot \vec{w}'_{n'h'} \, dy dy' = \sum_{m=1}^{M} \sum_{p=0}^{\infty} (\delta_l^m \delta_{n'}^m)^{p+1} \sigma_p^m \eta_{n'h'} \iint_{Y^m} \frac{b_{lk} T_p^m b'_{n'h'}}{\epsilon^m} \, dy dy'$$

$$\mathbf{R}_{\jmath\jmath'} = \sum_{m=1}^{M} \delta_n^m \delta_{n'}^m \iint_{Y^m} \vec{w}_{nh}^* \cdot \vec{G}^m(x_n, y, x_{n'}, y') \cdot \vec{w}'_{n'h'} \, dy dy' =$$

$$= \sum_{m=1}^{M} \left(\frac{\delta_n^m \delta_{n'}^m \eta_{nh} \eta_{n'h'} K_{nn'}^m}{\beta^2} \int_{Y^m} b_{nh} \mu^m b_{n'h'} \, dy + \sum_{p=0}^{\infty} \frac{(\delta_n^m \delta_{n'}^m)^{p+1} \sigma_p^m \nu_p^{m2}}{\beta_p^{m2}} \iint_{Y^m} \dot{b}_{nh} \, R_p^m \, \dot{b}'_{n'h'} \, dy dy' \right)$$

$$\mathbf{V}_{\imath r} = \delta_l^m \int_{Y^m} \vec{v}_{lk}^* \cdot \vec{e}_{pq}^{\,m}(x_l, y) \, dy = \begin{cases} \dfrac{(\delta_l^m)^{p+1} \beta_p^m}{\omega_{pq}'^m} \sqrt{\sigma_p^m} \displaystyle\int_{Y^m} \frac{b_{lk} \Psi_{pq}^m}{\epsilon^m} \, dy & \text{if } r \text{ corresponds to a LSM mode} \\ 0 & \text{if } r \text{ corresponds to a LSE mode} \end{cases}$$

$$\mathbf{W}_{\jmath r} = \delta_n^m \int_{Y^m} \vec{w}_{nh}^* \cdot \vec{e}_{pq}^{\,m}(x_n, y) \, dy = \begin{cases} \dfrac{(\delta_n^m)^{p+1} \eta_{nh} \beta_p^m}{\omega_{pq}'^m} \sqrt{\sigma_p^m} \displaystyle\int_{Y^m} \mu^m b_{nh} \Psi_{pq}^m \, dy & \text{if } r \text{ corresponds to a LSM mode} \\ -\dfrac{(\delta_n^m)^{p+1} \nu_p^m}{\beta_p^m} \sqrt{\sigma_p^m} \displaystyle\int_{Y^m} b_{nh} \, \Phi_{pq}^m \, dy & \text{if } r \text{ corresponds to a LSE mode} \end{cases}$$

where $b_{n0} = 1$, and:

$$\sigma_p^m = \begin{cases} 1/W^m & \nu_p^m = 0 \\ 2/W^m & \nu_p^m \neq 0 \end{cases} \qquad \eta_{nh} = \begin{cases} \kappa_n & \text{if } h = 0 \\ \beta & \text{if } h \neq 0 \end{cases} \qquad K_{nn'}^m = \begin{cases} \beta \operatorname{cosech}(\beta W^m) & \text{if } n \neq n' \\ \beta \operatorname{cotgh}(\beta W^m) & \text{if } n = n' \quad (\text{EWG}^m \text{of the type Fig. 3a}) \\ \beta \operatorname{tgh}(\beta W^m) & \text{if } n = n' \quad (\text{EWG}^m \text{of the type Fig. 3b,c}) \end{cases}$$

field representation up to the frequency $\omega_{\max}$. Therefore, the only meaningful eigenvalues are those larger than $\omega_{\max}^{-2}$.

The meaningful eigensolutions can be found using very efficient and reliable algorithms [15]. These eigensolutions yield the frequencies of all the modes that propagate below $\omega_{\max}$ with the given phase constant β. For each mode, $\boldsymbol{i}$ is obtained from (28) and, together with $\boldsymbol{q}$ and $\boldsymbol{a}$, permits the calculation of the modal field, using (21), (22), (5), (6), (2), and (3). It is noted that the normalizing condition

$$\tilde{\boldsymbol{q}} \boldsymbol{F} \boldsymbol{q} + \tilde{\boldsymbol{a}} \boldsymbol{a} = 1 \tag{34}$$

makes the modal magnetic field normalized to one, in the sense of the energy. In fact, the left-hand side of (34) and (33) are the same when $(\boldsymbol{q}, \boldsymbol{a})$ is en eigenvector of (29), so that the integral in (33) is equal to one.

III. NOTES ON THE NUMERICAL CODE AND RESULTS

a) Choice of the basis functions: The functions b_{nk} are first order (or triangular) splines. This choice results in a piece-wise linear approximation of J_y and in a piece-wise constant approximation of J_z and ρ. For simplicity, the singularities are approximated considering narrow splines placed at the points where the interfaces touch metallic or dielectric edges.

b) Calculation of $\omega_{pq}^{lm}, \omega_{pq}^{l'm}, \Psi_{pq}^m, \Phi_{pq}^m$: The resonant frequencies, that are the roots of the characteristic equations discussed at the end of Section II-A, are determined by the Newton method. The search of the roots is limited to the range (7). The determination of the eigenfunctions, that are represented in the form given in the Table II, reduces to the calculation of some coefficients known analytically.

c) Calculation of the matrix elements: This calculation requires the evaluation of a very large number of integrals (see Table III). This number is particularly large in the case of the matrices $\boldsymbol{F}, \boldsymbol{R}, \boldsymbol{T}$, and $\boldsymbol{S}$, since any term of the p-series involves a double integral. Fortunately, the form of the basis functions, of the eigenfunctions and of the Green's functions is simple enough for permitting the analytical evaluation of all integrals. Furthermore, most of the elementary integrals involved in the calculation are the same in many matrices. Therefore, evaluating all matrices in parallel the computation becomes much less cumbersome than it appears. The p-

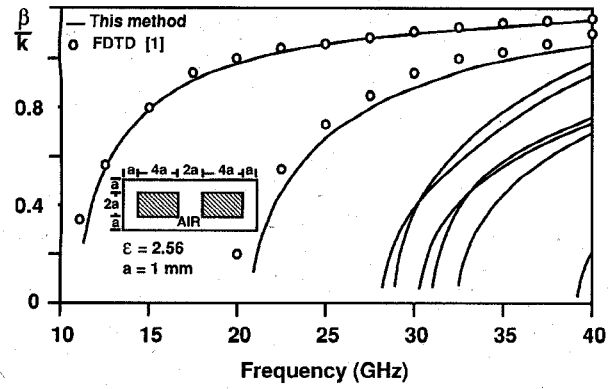

Fig. 4. Dispersion curves of the lower modes of two coupled dielectric waveguides.

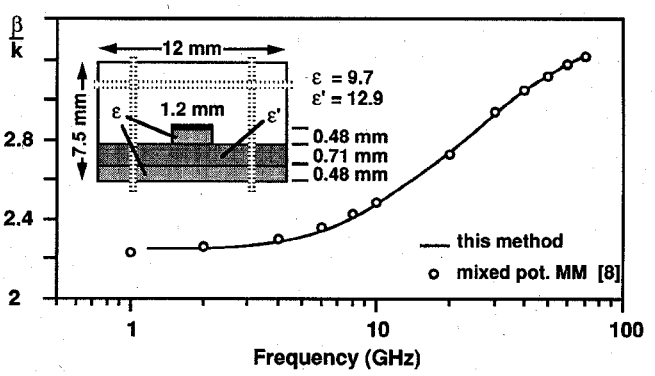

Fig. 5. Dispersion curve of the fundamental mode of a microslab line.

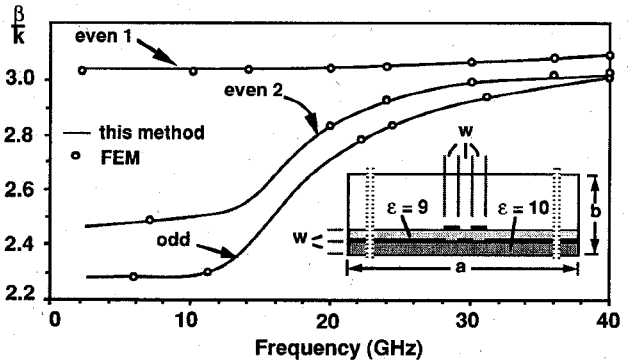

Fig. 6. Dispersion curves of the quasi-TEM modes of a multiconductor transmission line ($a = 5.75$ mm, $b = 2.5$ mm, $w = 0.25$ mm, and metallization thickness $= 0.25$ mm).

series are truncated when the relative correction due to the addition of the last term becomes smaller than a fixed amount Δ. In the cases of entries involving splines with nonoverlapping supports (i.e., in most cases), the integrals decrease exponentially with increasing p and the required precision in the evaluation of the series is reached after few terms. A larger number of terms is required in cases of overlapping splines, since in these cases the series converge more slowly, like p^{-2}.

d) Preliminary tests: A number of tests have been carried out using as benchmarks the dispersion characteristics of: *i)* the modes of a square waveguide, containing a homogeneous medium or a medium layered in the x- or y-direction only; *ii)* the TEM mode of a shielded stripline. The degeneracy of the modes of the square waveguide permitted us to verify the nonexistence of problems in cases of degeneracies; the stripline was considered to evidence possible problems caused by the imperfect representation of singularities at edges. The stability of the method has been tested by increasing the number of basis functions and the value of the parameter ζ (i.e., the number of the modes retained in the RME's) and by decreasing the error parameter Δ. No false convergence or spurious solution has been observed. These tests showed that, in all cases, fixing $\zeta = 2.5$ and $\Delta = 0.1\%$ was sufficient for obtaining an accuracy better than 1%, using a sufficient number of basis functions. Therefore these values were included in the code as defaults. Finally, we repeated many calculations subdividing the cross section into a number of EWG's larger than necessary, to see how much a large number of interfaces affects the accuracy of the results. No significant degradation was noted.

e) Results: We analyzed many structures considered in the literature, in order to compare our results with those obtained by other methods. In all cases the agreement was good and, in most cases, excellent.

Fig. 4 shows the dispersion of the first eight modes of two coupled dielectric waveguides surrounded by a conducting shield. The results for the first two modes are compared with the FDTD results reported in [1]. We calculated even and odd modes separately, placing a magnetic or electric wall at the symmetry plane. We used a total of $16 + 16$ splines in the two interfaces; the total number of resonant modes in the three EWG's was 27. Using a SUN Sparc10 workstation the CPU time for each class of symmetry was 9 sec, for a single value of β. This time is nearly the same as the CPU time required to find just two modes by the FDTD code [1], running on a similar workstation. Nearly all the CPU time was expended in the calculation of matrices $\boldsymbol{F}, \boldsymbol{R}, \boldsymbol{S}, \boldsymbol{T}$; in fact, the times required by the various steps were

computation of $\omega_{pq}^{\prime m}, \omega_{pq}^{\prime\prime m}, \Psi_{pq}^{m}, \Phi_{pq}^{m}$:	0.7%
computation of $\boldsymbol{V}, \boldsymbol{W}$:	0.3%
computation of $\boldsymbol{F}, \boldsymbol{R}, \boldsymbol{S}, \boldsymbol{T}$:	97%
solution of the eigenvalue problem:	1.6%
others:	0.4%

Fig. 5 shows the dispersion of the dominant mode of a shielded microslab waveguide [16], compared with the MM results reported in [8]. In this case we used 82 splines. The number of resonant modes was 87; this large number was a consequence of the large vertical size of the structure and of the high value of the maximum frequency of interest. Fig. 6 shows the dispersion of the quasi-TEM modes of a complicated three-conductor transmission line. Using the symmetry, $38 + 38$ splines were used on the two interfaces. The number of resonant modes was 26. Our results compare very well with FEM results obtained by a commercial package (2-D preprocessing of HFSS). With our method, however, the computing time decreased dramatically ($\approx$ 1/20).

IV. Conclusion

Admittedly, the method uses rather cumbersome formulas and, for this reason, its implementation in a computer code is a rather demanding job. Anyway, the result is a flexible, efficient, and reliable numerical tool, that compares favorably with other codes for the analysis of complex waveguides. The efficiency of the method depends not only on the reduced number of variables but also on its distinguishing feature of determining the propagating frequencies of the modes by solving a linear eigenvalue problem. This feature also contributes to the reliability of the method, especially in wideband analyses, since no risk exists of missing some eigenvalues. Another important reason for the reliability derives from the absence of spurious solutions, that affect almost all numerical methods for the solution of eigenvalue problems [17]. The zero-frequency spurious solutions that affected the early version of the method have been eliminated. The absence of other spurious solutions has been ascertained experimentally.

Appendix

A. Derivation of (10), (15), (16), and (17)

As discussed in [12] we have

$$\overleftrightarrow{G}^m = \sum_{pq} \vec{e}^m_{pq}(x,y)\vec{e}^{m*}_{pq}(x',y')/\omega^{m2}_{pq} \tag{35}$$

where the series includes all the LSM and LSE modes. Substituting (8) we obtain (10), where

$$S^m_p = \sum_{q=1}^{\infty} \frac{\Psi^m_{pq}(y)\Psi^m_{pq}(y')}{\omega'^{m4}_{pq}} \qquad R^m_p = \sum_{q=1}^{\infty} \frac{\Phi^m_{pq}(y)\Phi^m_{pq}(y')}{\omega''^{m2}_{pq}}$$

Introducing $T^m_p = \Sigma_q\, \Psi^m_{pq}(y)\Psi^m_{pq}(y')/\omega'^{m2}_{pq}$ it is easily verified that these expressions are the eigenfunctions expansions of the solutions of (15)–(17).

B. Positive Definiteness of $\boldsymbol{R}, \boldsymbol{S}$, and $\boldsymbol{F}$

Let us consider the quadratic form $U = \tilde{\boldsymbol{i}}\,\boldsymbol{R}\boldsymbol{i}$. Considering the first expression of $R_{jj'}$ given in Table III and using (35), we easily obtain

$$U = \sum_{m=1}^{M}\sum_{pq}\left|\sum_{j=1}^{H}\delta^m_n i^*_{nh}\int_{Y^m}\frac{\vec{w}^*_{nh}\cdot\vec{e}^m_{pq}}{\omega^m_{pq}}dy\right|^2 > 0 \quad \forall \boldsymbol{i} \neq 0.$$

Then $\boldsymbol{R}$ is positive definite. Along similar lines it can be shown that $\tilde{\boldsymbol{q}}\boldsymbol{S}\boldsymbol{q} > 0$ and $\tilde{\boldsymbol{q}}\boldsymbol{F}\boldsymbol{q} > 0 \forall \boldsymbol{q} \neq 0$ (positive definiteness of $\boldsymbol{S}$ and $\boldsymbol{F}$). For the demonstration we use the first expression of $\boldsymbol{S}_{ii'}$ and $\boldsymbol{F}_{ii'}$ given in Table III, and represent g and $\overleftrightarrow{G}$ in the form of eigenfunction expansion.

References

[1] S. Xiao, R. Vahldieck, and H. Jin, "Full-wave analysis of guided wave structures using a novel 2-D FDTD," *IEEE Microwave and Guided Wave Lett.*, vol. 2, pp. 165–167, May 1992.

[2] F. Arndt, V. J. Brancovic, and D. V. Krupezevic, "An improved FD-TD full-wave analysis for arbitrary guiding structures using a two-dimensional mesh," in *IEEE MTT-S Int. Symp. Dig.*, June 1992, pp. 389–392.

[3] A. Asi, L. Shafai, "Dispersion analysis of anisotropic inhomogeneous waveguides using compact 2-D-FDTD," *Electron. Lett.*, vol. 28, pp. 1451–1452, July 16, 1992.

[4] D. V. Krupezevic, V. J. Brankovic, and F. Arndt, "The wave-equation FD-TD method for efficient eigenvalue analysis and S-matrix computation of waveguide structures," *IEEE Trans. Microwave Theory Tech.*, vol. 41, pp. 2109–2115, Dec. 1993.

[5] A. C. Cangellaris and W. Pinello, "Dispersion analysis of multiconductor waveguiding systems using point-matched time-domain finite elements," in *Proc. 2nd Int. Workshop Finite Element Methods for Electromagnetic Wave Problems,* Siena, May 1994, COMPEL, vol. 13, Suppl. A, pp. 243–248.

[6] H. Jin and R. Vahldieck, "Full-wave analysis of guiding structures using a 2-D array of 3-D TLM nodes," *IEEE Trans. Microwave Theory Tech.*, vol. 41, pp. 472–77, Mar. 1993.

[7] M. Celuch-Marcysiak and W. K. Gwarek, "A transformed symmetrical condensed node for the effective TLM analysis of guided wave problems," *IEEE Trans. Microwave Theory Tech.*, vol. 41, pp. 820–23, May 1993.

[8] Ching-Kuang, C. Tzuang, and Jan-Dong Tseng, "A full-wave mixed potential mode matching method for the analysis of planar or quasi-planar transmission lines," *IEEE Trans. Microwave Theory Tech.* vol. 39, pp. 1701–1711, Oct. 1991.

[9] M. Swaminathan, T.K. Sarkar, and A.T. Adams, "Computation of TM and TE modes in waveguides based on surface integral formulation," *IEEE Trans. Microwave Theory Tech.*, vol. 40, pp. 285–297, Feb. 1992.

[10] F. Olyslager and D. De Zutter, "Rigorous boundary integral equation solution for general isotropic and uniaxial anisostropic dielectric waveguided in multilayered media including losses, gain and leakage," *IEEE Trans. Microwave Theory Tech.*, vol. 41, pp. 1385–1392, Aug. 1993.

[11] W. Schroeder and I. Wolff, "Full-wave boundary integral analysis of integrated transmission lines: Origin and avoidance of spurious solutions," in *Proc. 20th European Microwave Conf.*, Budapest, Sept. 1990, pp. 829–834.

[12] M. Bressan, G. Conciauro, and P. Gamba, "A new method for numerical modeling of general quasiplanar waveguides," in *Proc. Int. URSI Symp. Electromagnetic Theory*, Sydney, Aug. 17–20, 1992, pp. 342, 344.

[13] ——, "A new method for the analysis of integrated transmission lines," *Annales des Télécommunications*, vol. 47, no. 11–12, pp. 548–550, Nov–Dec. 1992.

[14] M. Bressan and P. Gamba, "Analytical expressions of field singularities at the edge of four right wedges," *IEEE Microwave and Guided Wave Lett.*, vol. 4, pp. 3–5, Jan. 1994.

[15] E. Anderson *et al.*, *LAPACK, User's Guide*, SIAM, Philadelphia, 1992.

[16] B. Young and T. Itoh, "Analysis and design of microslab waveguide," *IEEE Trans. Microwave Theory Tech.*, vol. 35, pp. 850–857, Sept. 1987.

[17] W. Schroeder and I. Wolff, "The origin of spurious solutions in numerical solution of electromagnetic field eigenvalue problems," *IEEE Trans. Microwave Theory Tech.*, vol. 42, pp. 644–653, Apr. 1994.

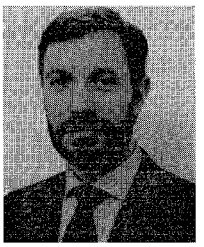

Marco Bressan (M'93) was born in Venice, Italy, in 1949. He received the degree in electronic engineering from the University of Pavia in 1972.

Since 1973 he has been with the Department of Electronics of the University of Pavia, as a Researcher in the field of electromagnetics. In 1987, he joined the Faculty of Engineering of the University of Pavia, where currently he teaches Antennas and Propagation as an Associate Professor. His main research interests are in antenna theory and analytical and numerical techniques for electromagnetics. At present, he is responsible for the formulation of numerical general algorithms for the wide band analysis of 3-D passive microwave circuits including homogeneous or stratified media.

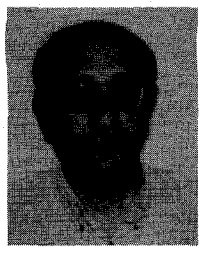

Giuseppe Conciauro (A'72–M'93) was born in Palermo, Italy, in 1937. He received a degree in electrical engineering from the University of Palermo, Italy in 1961, and the "Libera Docenza" in electronics in 1971.

Since 1963 to 1971 he has been with the Institute of Electrical Engineering of the University of Palermo as an Assistant Professor of microwave theory. In 1971 to 1980, he was with the Department of Electronics of the University of Pavia, Italy, where he has taught microwave theory as an Associate Professor. He is also teaching electromagnetic theory at the same University as a Full Professor. From 1985 to 1991 he served as Director of the Department of Electronics of the University of Pavia. His main research interests are in microwave theory, interaction structures for particle accelerators and numerical methods in electromagnetics.

Dr. Conciauro is a member of AEI and on the Editorial Board of the IEEE TRANSACTIONS ON MICROWAVE THEORY AND TECHNIQUES.

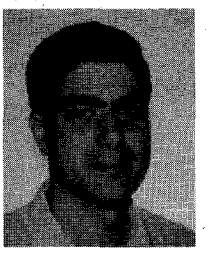

Paolo Gamba (S'90–M'94) was born in Cremona, Italy, in 1965. He received the Laurea degree in electronic engineering "cum laude" from the University of Pavia, Italy, in 1989. He also received the Ph.D. degree in electromagnetics in 1993 from the same University.

From 1992 to 1994 he was an R&D engineer in the Microwave Laboratory of Siemens Telecomunicazioni, Cassina de' Pecchi, Milano, Italy, where he was involved in numerical modeling of waveguide components. In 1994, he joined the Department of Electronics of the University of Pavia as a Researcher in Electromagnetics. His current research interests include the development of numerical models for the analysis of transmission lines and millimeter-wave integrated circuits, and remote sensing and multidimensional signal processing.